PCCP

PAPER

View Article Online
View Journal

Cite this: DOI: 10.1039/d6cp00104a

Polyol-based deep eutectic solvents: betaine *versus* choline chloride

Gabriel Teixeira,[a] Dinis O. Abranches,[a] Gangqiang Yu,[bc] Christoph Held,[b] Luís M. N. B. F. Santos,[d] Olga Ferreira*[e] and João A. P. Coutinho[a]

This work investigates the potential of betaine as a substitute for choline chloride in the formation of polyol-based DES. The solid–liquid equilibrium (SLE) phase diagrams of binary mixtures of betaine with one polyol (ethylene glycol, 1,3-propanediol, glycerol, *meso*-erythritol, xylitol, or sorbitol) were studied across the entire composition range. Experimental measurements of the phase diagrams were limited by the thermal degradation of betaine and by the boiling points or high viscosities of some polyols. Overall, betaine exhibited negative deviations from ideality, while most polyols displayed near-ideal behaviour. COSMO-RS, a thermodynamic model, satisfactorily predicts these deviations from ideality and the observed phase behaviour. Mixtures of betaine and polyols yielded a narrower liquid-phase window for room-temperature applications than the corresponding choline chloride systems. The cross-association of betaine with polyols is more favourable than its self-association, and stronger interactions between the polyols and betaine than with choline chloride are expected, leading to more negative deviations; thus, the smaller melting temperature depression must result from a higher enthalpy of fusion of betaine than that of choline chloride.

Received 11th January 2026,
Accepted 5th May 2026

DOI: 10.1039/d6cp00104a

rsc.li/pccp

1. Introduction

Since the seminal article by Abbott *et al.* (2003), deep eutectic solvents (DES) have received increasing attention. These highly tuneable solvents are usually formed by combining two or more compounds that cross-associate, that is, between hydrogen bond donors (HBD) and acceptors (HBA). To be considered "deep" melting point depressions, these interactions should lead to mixtures with lower melting points than those of an ideal mixture.[1,2]

Among the organic salts studied for the formation of DES, choline chloride (ChCl) is the most frequently used.[3–8] This biodegradable quaternary ammonium salt is viewed as an exceptional DES-forming component due to its HBA capabilities,[9–11] and low cost and toxicity.[12–14] In addition, it has a low estimated melting enthalpy.[15–19] Despite all the advantages, commercial ChCl is chemically synthesised,[20] not very chemical or thermally stable, and its DES are not halogen-free mixtures.

Recently, betaine has been studied as a promising HBA substitute for ChCl in DES.[2,19] It is a biodegradable, halogen-free zwitterion derived from renewable sources. Additionally, its structure contains a strong anionic carboxylate moiety, while the ammonium moiety is partially protected by methyl groups, preventing betaine from forming strong self-association interactions.[19] However, it has a higher estimated melting enthalpy than ChCl (17.98 kJ mol^{-1} *vs.* 4.3 kJ mol^{-1}), and both degrade upon melting.[15,21]

Hansen *et al.*[22] have reviewed the main prospective applications of DES in diverse areas, including metallurgy and electrodeposition, separations and gas capture, power systems and battery technology, biocatalysis and organic chemistry, biomass processing, biomolecular structure, folding, and stability, pharmaceuticals and medical research, or nanomaterials synthesis. While ChCl mixtures have been used across all these areas, betaine-based DES have been much less studied. However, relevant applications can be cited in biomass pretreatment,[23] extraction processes of target compounds from natural matrices,[24,25] and as media to increase enzyme stability.[26]

It is important to note that most of these studies use DES prepared at a specific molar ratio of its components, often containing water, to ensure they remain in the liquid phase for

[a] *CICECO – Aveiro Institute of Materials, Department of Chemistry, University of Aveiro, Campus Universitário de Santiago, Aveiro, Portugal*
[b] *Laboratory of Thermodynamics, Department of Biochemical and Chemical Engineering, TU Dortmund University, Emil-Figge-Street 70, Dortmund 44227, Germany*
[c] *Faculty of Environment and Life, Beijing University of Technology, 100 Ping Le Yuan, Chaoyang District, Beijing, 100124, China*
[d] *CIQUP, Institute of Molecular Sciences (IMS), Department of Chemistry and Biochemistry, Faculty of Science, University of Porto, Rua do Campo Alegre, Porto 4169-007, Portugal*
[e] *CIMO, LA SusTEC, Instituto Politécnico de Bragança, Campus de Santa Apolónia, 5300-253 Bragança, Portugal. E-mail: oferreira@ipb.pt*

a given application. This approach overlooks the causes of negative deviations from the thermodynamic behaviour typical of deep eutectic mixtures, limiting the development of new applications across broader temperature and composition ranges. The complete solid–liquid equilibria (SLE) phase diagrams should be studied to achieve a more comprehensive molecular-level understanding of DES formation, while providing the liquid-phase window of compositions.

This work addresses the use of betaine as a substitute for choline chloride in selected DES by studying their SLE phase diagrams over the full composition range. Betaine should fill the role of an HBA even better than ChCl, since it is a lone HBA. In other words, betaine has a strong HBA dual site (COO^- moiety) but no relevant HBD capabilities (methyl groups shield its formal positive charge), preventing betaine–betaine hydrogen bonding. ChCl, on the other hand, can easily hydrogen bond with itself through the OH group of the choline cation and the chloride anion. Thus, ChCl is significantly less available to serve as an HBA in DES mixtures than betaine. Complementarily, polyols are promising candidates for an HBD,[27] being one of the most relevant families of compounds studied in DES.[22] The SLE phase diagrams of binary mixtures of betaine with polyols (ethylene glycol, 1,3-propanediol, glycerol, *meso*-erythritol, and xylitol) will be studied experimentally and compared with those reported by Silva *et al.*[28] To assist in the discussion and evaluation of the non-ideality of the systems studied, the fully predictive Conductor-like Screening Model for Real Solvents (COSMO-RS) model will be used.[29–32]

2. Materials and methods

2.1. Chemicals

The CAS number, supplier, purity, melting temperature (T_m), melting enthalpy ($\Delta_m H$), and difference between the molar heat capacity of the liquid and solid phases ($\Delta_m c_P$) of the compounds studied in this work are listed in Table 1. The melting properties of betaine were estimated using a group contribution method.[21]

2.2. Solid–liquid equilibria measurement

The phase diagrams were determined experimentally using three techniques: the visual capillary method, the visual flask method, and differential scanning calorimetry (DSC). The visual capillary method was used exclusively for mixtures that were mostly or completely solid at room temperature, with or without prior melting. Measurements were taken using an automatic glass capillary device (Büchi model M565) with a temperature resolution of 0.1 K. For each sample, at least three independent measurements were performed, at a heating rate of 0.2 K min^{-1}. For mixtures with a pasty consistency, the visual flask method was employed. Samples (approximately 1 g of the mixture) were heated in a custom-made aluminium heating block under continuous stirring until they were completely melted. The melting temperatures, recorded with a Pt100 probe accurate to $\pm$0.1 K, were defined as the point at which the last solid particle disappeared.

DSC proved valuable for measuring phase transitions in mixtures that did not fully crystallise at room temperature and for determining the corresponding enthalpies. Samples weighing between 5 and 25 mg were measured using a Perkin-Elmer AD6 micro-analytical balance (with an accuracy of $\pm$0.006 mg) and sealed in hermetic aluminium crucibles. Measurements were conducted with a DSC Hitachi model DSC7000X, operating at atmospheric pressure and coupled to an electrical cooling unit. A baseline was established with an empty sample holder to eliminate the effect of the gas on the sample holders. The equipment was calibrated using thirteen standards (decane, 4-nitrotoluene, naphthalene, benzoic acid, diphenylacetic acid, indium, tin, caffeine, lead, zinc, potassium nitrate, water, and anthracene) at a heating rate of 2 K min^{-1}. All measurements were performed in heating mode at the same rate to ensure consistency. Samples in a liquid state that presented a ''resistance'' to recrystallisation were subjected to a special heat treatment before the final melting step. This involved at least two heating (at 2 K min^{-1}) and cooling (at 5 K min^{-1}) cycles to ensure partial or complete crystallisation, which was not always apparent. Finally, the last heating step was performed for thermal analysis until complete melting.

2.3. Solid–liquid equilibria modelling

Assuming pure solid phase and neglecting the effect of temperature on the heat capacities difference, the solid–liquid equilibria can be described by eqn (1),

$$\ln(x_i\gamma_i) = \frac{\Delta_m H}{R}\left(\frac{1}{T_m} - \frac{1}{T}\right) + \frac{\Delta_m c_P}{R}\left(\frac{T_m}{T} - \ln\frac{T_m}{T} - 1\right) \quad (1)$$

where γ_i is the activity coefficient of compound i at mole fraction x_i in a solution, $\Delta_m H$ and T_m are the melting enthalpy and temperature of pure compound i at the temperature of

Table 1 Source, purity and melting properties of the studied compounds

Compound	Source	CAS	Purity[a] wt%	T_m/K	$\Delta_m H$/kJ mol^{-1}	$\Delta_m c_P$[b]/J K^{-1} mol^{-1}
Betaine	Alfa Aesar	107-43-7	>98%	566.2[21]	17.98[21]	—
Ethylene glycol	Sigma-Aldrich	107-21-1	>99.5%	260.8[33]	11.6[33]	47.1[33,34]
1,3-Propanediol	Sigma-Aldrich	504-63-2	>98%	249[35]	11.4[35]	56.6[34]
Glycerol	Biochem–Frilabo	56-81-5	Analytical reagent	293[36]	18.28[36]	68.1[37,38]
meso-Erythritol	Alfa Aesar	149-32-6	>99%	391.2[39]	38.9[39]	115.6[40]
Xylitol	Acros Organics	87-99-0	>99%	365.7[41]	37.40[41]	142.8[42]
Sorbitol	Panreac	50-70-4	>97%	366.5[41]	30.20[41]	204.7[43]

[a] Declared by the supplier. [b] Heat capacity differences calculated with experimental data of the solid and liquid phase heat capacities.

melting, T_m, R is the universal gas constant (J K^{-1} mol^{-1}), T is the absolute temperature, and $\Delta_m c_P$ is the difference between the molar heat capacity of compound i in the liquid and solid phases. eqn (1) was used to describe the SLE of the polyols. Due to the unavailability of $\Delta_m c_P$ data for betaine, the second term of eqn (1) is usually disregarded for this compound.[1,44] This simplification results in eqn (2):

$$\ln(x_i\gamma_i) = \frac{\Delta_m H}{R}\left(\frac{1}{T_m} - \frac{1}{T}\right) \quad (2)$$

For choline chloride, eqn (2) was also applied using the melting properties (T_m = 597 K, ΔH = 4.3 kJ mol^{-1}) proposed by Fernandez *et al.*,[15] and for betaine, the values proposed by Wang *et al.*[21] (T_m = 566.2 K, ΔH_m = 17.98 kJ mol^{-1}).

2.4. The COSMO-RS model and conformer optimisation

COSMO-RS is a fully predictive thermodynamic model that estimates the chemical potential and activity coefficient of each component in a liquid mixture by combining statistical thermodynamics with quantum chemical descriptors of the molecules.[29,30,45,46] It uses density functional theory (DFT) calculations to obtain σ-surfaces, where the geometry of each molecule is optimised by embedding it in a continuum solvent, on top of which screened charges (σ) are calculated.[47] Activity coefficients predicted using COSMO-RS were combined with eqn (1) and (2) in an iterative workflow to calculate the SLE phase diagram of each system. The melting properties of the studied compounds are listed in Table 1. The geometry of the compounds and their corresponding σ-surfaces were either generated using COSMOconfX 2021 software,[48] which optimises the conformers using TURBOMOLE V7.4 2019[49,50] with DFT and the BP-86 functional, the def_TZVP or def2_TZVPD basis sets, and the COSMO solvation model with infinite permittivity (1,3-propanediol, *meso*-erythritol, xylitol, and sorbitol), or obtained from the original database of COSMOtherm[51] (ethylene glycol and glycerol). Finally, the COSMOtherm[51] software package with the BP_TZVP_21 and BP_TZVPD_FINE_21 parametrisations was used. The conformers obtained through either approach were used in the calculations. Their Sigma profiles are shown in Fig. S1 of the SI.

3. Results and discussion

3.1. Binary systems of betaine and polyols

The SLE phase diagrams of betaine with ethylene glycol, 1,3-propanediol, glycerol, *meso*-erythritol, or xylitol, measured in this work (experimental data reported in Tables S1 to S5, in SI), along with data reported in the literature for systems of betaine and ethylene glycol,[21,52] xylitol,[53] or sorbitol,[19] are presented in Fig. 1.

The experimental phase diagrams present a single eutectic point, except for the betaine and ethylene glycol system, which exhibits cocrystal formation. This phase diagram is in good agreement with the literature data,[21,52] and the measurements reported here suggest the presence of an incongruent cocrystal formation (peritectic transition). Unfortunately, further characterisation of this cocrystal was not possible in this work, but future studies should be carried out by X-ray Powder Diffraction (XRPD) to confirm the stoichiometry of these suspected cocrystals. The formation of betaine cocrystals with phenolic compounds and weak organic acids has been previously reported.[54,55] These cocrystals are established mainly through hydroxyl-carboxylate interactions.

As expected, the mixtures with 1,3-propanediol and glycerol exhibited higher viscosity than those with ethylene glycol, making measurements using the visual flask method and DSC more difficult. Nonetheless, the mixtures with melting temperatures above room temperature of these three systems rarely (partially) recrystallise after the first complete melting. Therefore, the results obtained are either the temperature of disappearance of the last crystal of betaine (in the visual flask method) or the endothermic transition observed in the DSC thermogram after extensive thermal treatment, as described in Section 2.2. This ''resistance'' to recrystallisation was also observed, although to a lesser extent, in the mixtures of *meso*-erythritol, xylitol, and sorbitol.

In the case of the betaine and xylitol phase diagram, the solidus and liquidus lines measured in this work do not match, as the eutectic temperature measured was 335 ± 4 K, and the lowest melting temperature, at $x_{betaine}$ = 0.20, was 358.5 ± 1.0 K, a difference of 24 K. Interestingly, early literature[56] reports two crystalline forms of xylitol: a metastable, monoclinic and hygroscopic form that melts at 334 K, and the stable orthorhombic form melting at 367 K. Additionally, our phase diagram does not agree with the literature data of Palmelund *et al.*,[53] which reported a lower eutectic temperature (309.5 K). To investigate the reason behind such discrepancies, the influence of water in these diagrams will be discussed later. On the other hand, the betaine–sorbitol mixture measurements show a phase behaviour suggesting the possibility of cocrystal formation (a peritectic point at approximately a mole fraction of 0.7).

Fig. 1 also shows the ideal liquidus lines of betaine calculated using eqn (2) with γ_i = 1, and the melting properties proposed by Wang *et al.*:[21] the melting enthalpy of 17.98 kJ mol^{-1} estimated using a group contribution method, and the melting temperature of 566.2 K measured by DSC. To our knowledge, there are no other measurements or estimates of these values. Additionally, the experimental activity coefficients for these systems are presented in Fig. 2 along with the COSMO-RS predictions.

As shown in Fig. 2, all polyols exhibited ideal or nearly ideal behaviour, whereas betaine displayed negative deviations in all mixtures. This behaviour is expected given the molecular structures of the compounds studied. Polyols, with their multiple hydroxyl groups, already form strong hydrogen-bonding networks in their pure phases. Thus, polyol–betaine interactions are not significantly stronger than polyol–polyol interactions, leading to thermodynamic behaviour near ideality in the narrow composition range available. In stark contrast, betaine–betaine interactions are much less favourable than polyol–betaine interactions (hydrogen bonding), leading to betaine displaying strong negative deviations from ideality.

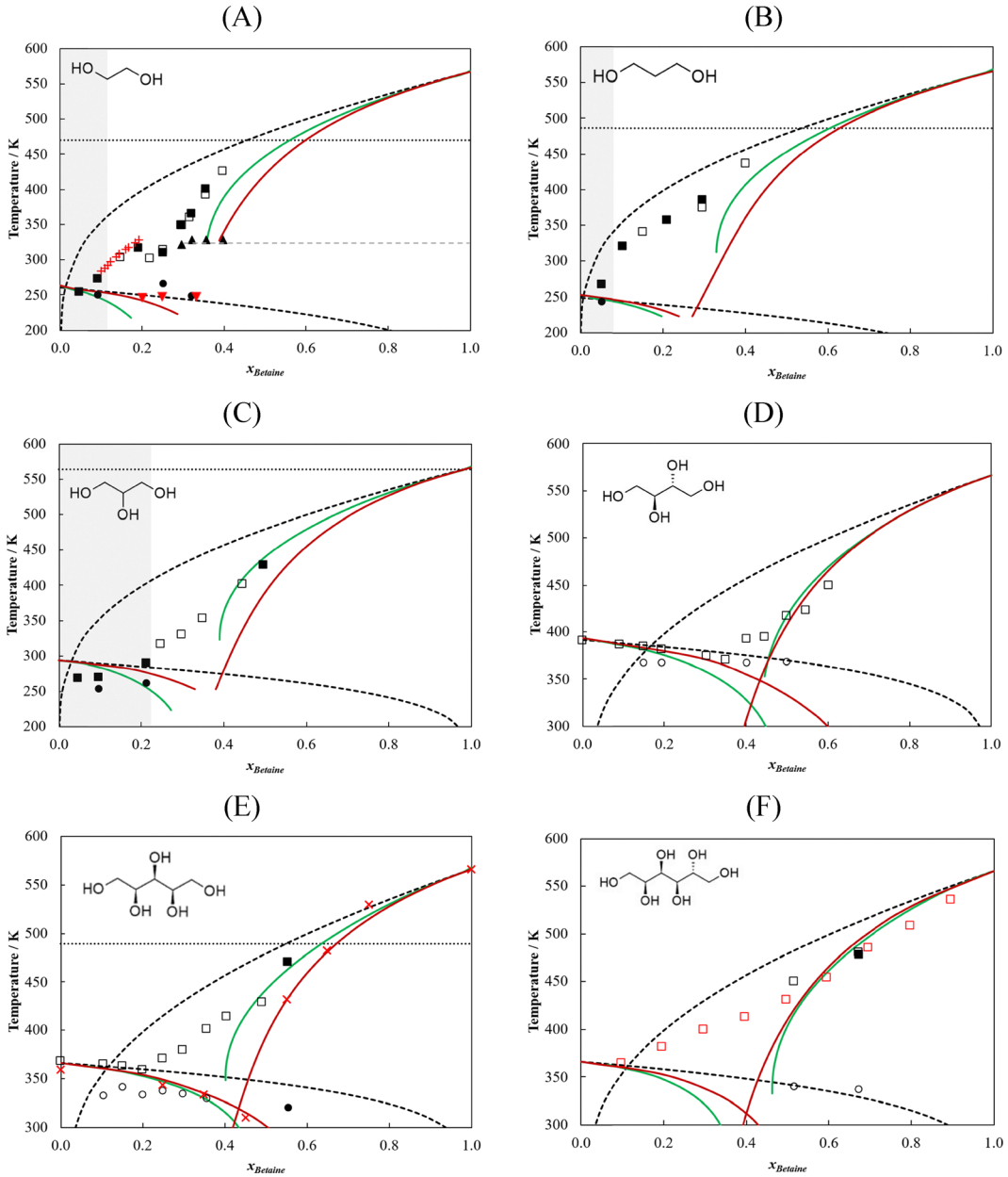

Fig. 1 Solid–liquid phase diagrams of binary mixtures composed of betaine and (A) ethylene glycol, (B) 1,3-propanediol, (C) glycerol, (D) *meso*-erythritol, (E) xylitol, and (F) sorbitol. Symbols represent experimental melting temperatures (□, ■), eutectic temperatures (●, ○), and other transitions (▲), measured using the visual capillary or flask method (open symbols) or DSC (black symbols), and data from Wang *et al.* (+),[21] Palmelund *et al.* (×),[53] Mero *et al.* (▼),[52] and Abranches *et al.* (□).[19] Lines represent the ideal model (- - -), COSMO-RS TZVP parametrisation (—), COSMO-RS TZVPD-FINE parametrisation (—) and polyol normal boiling temperature (···). The grey region represents the concentration range of a stable monophasic liquid phase at room temperature.

Notwithstanding the previous paragraph and the molecular interpretation of the results reported in Fig. 2, the experimental activity coefficients of betaine, calculated using eqn (2) are, unlike those for the polyols, dependent on the melting properties of betaine, which introduces a significant uncertainty in these values. Because these properties are estimated (rather than directly and rigorously experimentally measured), the experimental betaine activity coefficients must be interpreted with care and only in a qualitative (rather than strictly quantitative) manner. Nevertheless, the activity coefficients predicted by COSMO-RS, calculated at the experimental T and $x_{betaine}$ conditions, are independent of the melting properties. These predicted activity coefficients are in perfect qualitative agreement with the experimental values, supporting the conclusion that betaine exhibits strong negative deviations from ideality. The same trend is observed in the predicted isothermal activity coefficients, at 300 K and 400 K, in Fig. S2 (plots A and C).

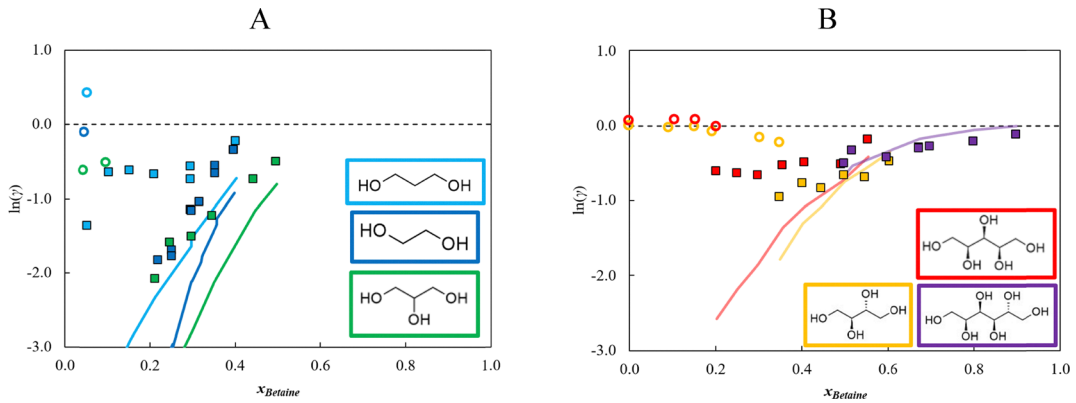

Fig. 2 Non-isothermal experimental activity coefficients of betaine (square) and the polyols (circle) of 1,3-propanediol, ethylene glycol, and glycerol (plot A), and *meso*-erythritol, xylitol, and sorbitol (plot B), calculated using eqn (2) with ΔH_m = 17.98 kJ mol^{-1} and T_m = 566.2 K. The black dashed line represents the ideal behaviour. The solid lines represent the activity coefficients predicted by COSMO-RS (TZVPD-FINE parametrisation), calculated at the experimental T and $x_{Betaine}$ conditions. Colour code: 💧, 1,3-propanediol; 💧, ethylene glycol; 💧, glycerol; 💧, *meso*-erythritol; 💧, sorbitol; 💧, xylitol.

Given that betaine displays negative deviations from thermodynamic ideality, its ideal liquidus line must be above (*i.e.*, at a higher temperature) than its experimental counterpart. This can be used to establish a lower boundary for the melting enthalpy of betaine by plotting $\ln(x_{betaine})$ as a function of $1/T$ for the six mixtures (see Fig. S3). The slope of these plots provides a direct estimate of the enthalpy of dissolution of betaine ($-\Delta_{diss}H/R$). Since

$$\Delta_{diss}H(T) = \Delta_m H(T) + H^E(T)$$

and considering that there are negative deviations from ideality and thus H^E is negative, the enthalpy of dissolution, represents the lower boundary of the melting enthalpy. This value is set to 12.0 kJ mol^{-1} (the value obtained from the higher negative slope for the betaine and ethylene glycol system). It should be borne in mind that the $\Delta_m c_P$ contribution and potential solid–solid transitions are not being considered to estimate the value of $\Delta_m H(T_m)$.

As stated above, the negative deviations of betaine stem from the fact that its cross-association interactions with polyols are stronger than its self-association. Examining the zwitterion's structure, the methyl groups hinder the positive charge, preventing strong ion–ion interactions with its carboxylate anion. Its weak HBD and strong HBA capabilities are consistent with the Sigma profile and surface predicted by COSMO-RS using the TZVPD-FINE parametrisation, as shown in Fig. S1. When mixed with polyols, favourable cross-interactions occur between the carboxylate group of betaine and the HBD sites of the polyols. For the polyols studied, betaine shows slightly stronger cross-interactions with ethylene glycol and glycerol than with the other polyols, as shown in Fig. 2.

Regarding the descriptive capabilities of COSMO-RS of the phase diagrams, Fig. 1 presents the model's predictions using the TZVP and TZVPD-FINE parametrisations. Overall, the betaine-rich regions of the diagrams are qualitatively well described by the model, especially with the TZVP parametrisation. We can only reasonably evaluate the model's ability to represent the polyol melting temperatures in the *meso*-erythritol, xylitol, and sorbitol systems, since this window is narrower for the other polyols, where the TZVPD-FINE parametrisation offers slightly better descriptions.

3.2. The impact of water in betaine phase diagrams

Betaine is a hygroscopic compound; therefore, it is very relevant to investigate how the phase diagrams of binary mixtures containing betaine compare to the sometimes unintentionally obtained ternary mixture of betaine/second compound/water. Abranches *et al.* (2020)[19] previously studied the effect of adding 2 wt% of water to the betaine/sorbitol, betaine/menthol, and betaine/urea mixtures. This weight fraction corresponds to average water mole fractions of 15% for betaine/sorbitol, 13% for betaine/menthol, and 9% for betaine/urea. Among these three pseudo-binary systems, betaine/urea/water showed the most significant difference from its binary counterpart,[57] followed by the sorbitol and menthol systems. The considerable decrease in melting temperatures of the betaine/urea/water system was justified by demonstrating that the molecular interactions between betaine and urea were significantly enhanced in the presence of water, with DFT simulations supporting the validation of their hypothesis.[57]

Similarly, several betaine/xylitol/water mixtures were prepared. However, only three recrystallised, two at 5%, and one at 11% water mole fraction. These mole fractions correspond to 0.6 wt% and 1.6 wt% of water, respectively. The SLE measurements of these mixtures, along with the experimental activity coefficients, are shown in Fig. 3. The binary and pseudo-binary systems containing sorbitol were adapted from Abranches *et al.*,[19] and added to Fig. 3. Detailed experimental data and their activity coefficients are presented in Table S6.

The data measured with a 5% water mole fraction matches the data obtained by Palmelund *et al.*,[53] which suggests that their mixtures have similar water content; nonetheless, the decrease in eutectic temperature with such a small amount of water (about 0.6 wt%) is remarkable. This implies that a small amount of water is sufficient to strengthen the hydrogen bond network in the liquid phase, significantly lowering the melting

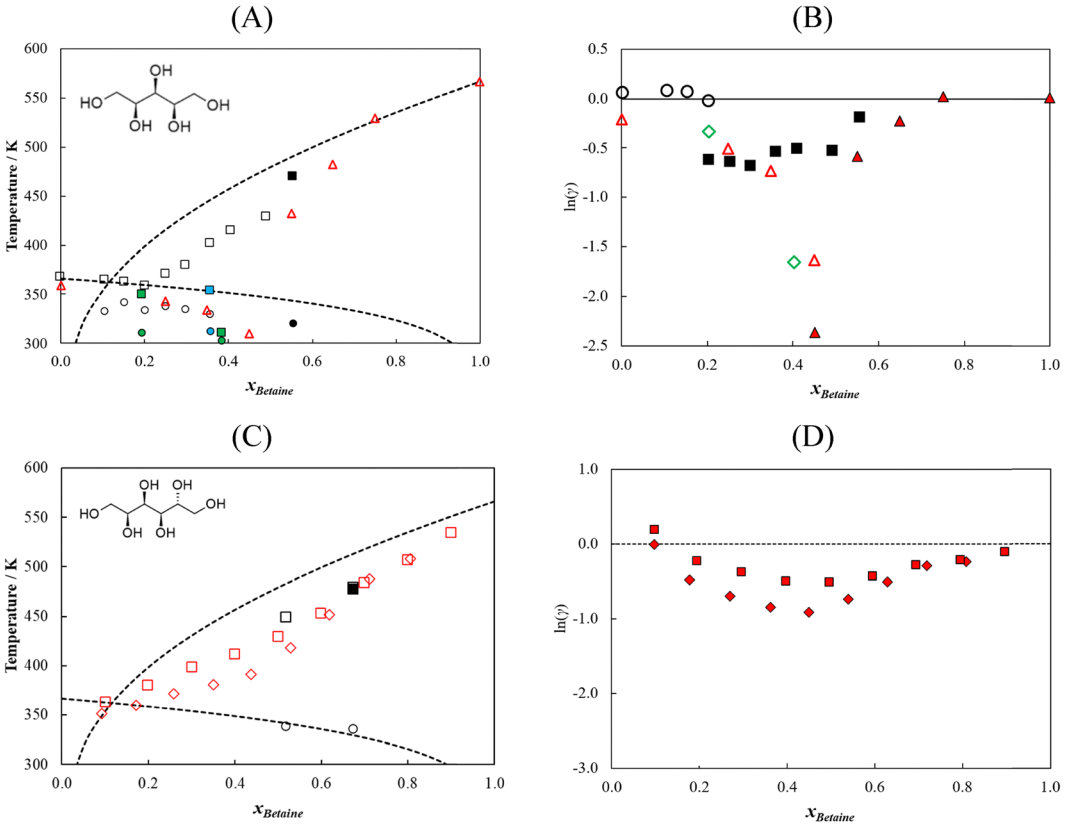

Fig. 3 Solid–liquid phase diagrams of (A) betaine/xylitol and (C) betaine/sorbitol,[19] and non-isothermal activity coefficients (B) and (D) of betaine (filled symbol) and the polyol (open symbol). Symbols in (A) and (B) present data without added water (black symbols), with 0.6 wt% (green symbols), and 1.6 wt% (blue symbols) added water, and data from the literature,[53] in (C) and (D) represent data without added water (red squares) and 2 wt% (red diamond) added water. The *x*-axis is the mole fraction of betaine in the ternary systems. Lines in (A) and (C) represent the ideal model and in (B) and (D) represent the ideal behaviour, $\ln(\gamma_i) = 0$.

temperature and, consequently, the eutectic temperature. Such a difference in phase behaviour can be explained if the most representative conformers of xylitol in water mixtures differ from those in anhydrous mixtures. In the presence of water, xylitol conformers likely have an increased ability to form cross-hydrogen bonds with water. In contrast, in the absence of water, they tend to have stronger intramolecular interactions. This change has already been studied,[58] showing that the number of hydrogen bonds water can form with dissolved polyols is lower, but not significantly different from those in pure water. These water–water interactions are likely replaced by water–polyol interactions, indicating a more cross-interacting polyol conformer.

Despite that, the reason the 11% water mole fraction measurement shows a higher melting temperature than the 5% remains unclear. A hypothesis is the presence of the betaine monohydrate. In sorbitol binary and pseudo-binary systems, the presence of water lowers the melting temperatures of the ternary system relative to its binary counterpart. However, this decrease was not as impressive as in the xylitol mixtures, especially with 0.6 wt%. Since the water weight fraction of both polyol ternary mixtures is similar (for the 1.6 wt% of water in the xylitol mixture), the formation of betaine monohydrate may also affect this phase diagram. To support this assumption, the phase diagrams of betaine monohydrate with both glycerol and xylitol from the literature[53,59] are shown in Fig. S4, showing higher melting temperatures than those in mixtures with anhydrous betaine or low amounts of water. Further investigation is needed to determine the crystallography of the solid phase of these mixtures, including those that do not appear to be affected by monohydrate formation, such as the betaine/urea/water mixture.[60]

3.3. Comparison with choline chloride

The SLE phase diagrams of the polyols with betaine or choline chloride are compared in Fig. 4, and the corresponding activity coefficients are shown in Fig. 5. The SLE phase diagram of betaine and sorbitol,[19] and choline chloride with all polyols[28] were taken from the literature.

Silva *et al.*[28] observed that, in general, the ChCl solubility curve exhibited a near-ideal behaviour, indicating that the temperature depression was due to its low melting enthalpy rather than any specific cross-interactions. This behaviour is expected, as the primary cross-interactions in ChCl/polyol systems likely involve the hydroxyl groups of the polyols interacting with the chloride anion. This interaction is already present in pure ChCl, where the hydroxyl group of the cation can interact with the chloride anion. In contrast, the negative

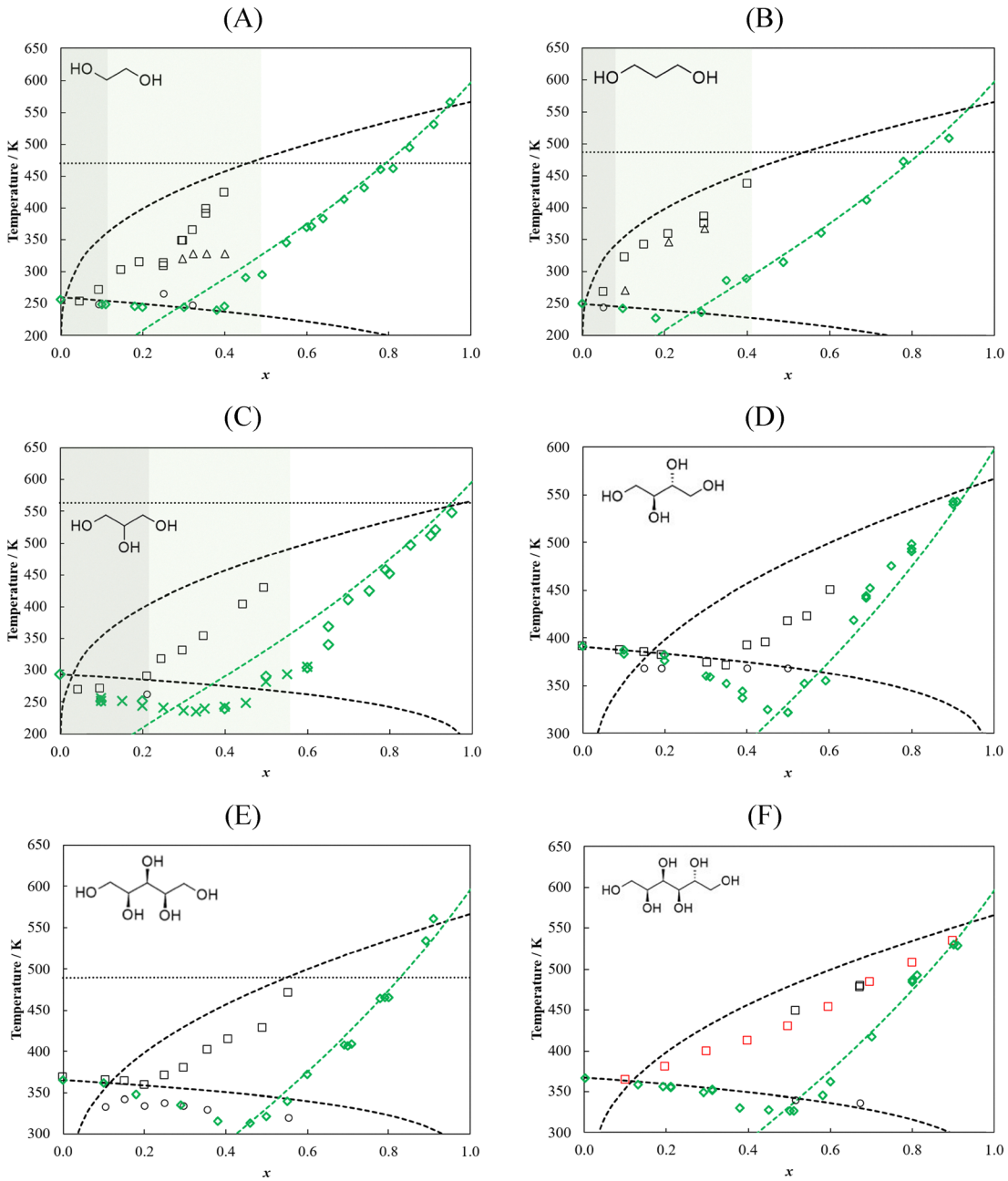

Fig. 4 Solid–liquid phase diagrams of binary mixtures composed of betaine or choline chloride and (A) ethylene glycol, (B) 1,3-propanediol, (C) glycerol, (D) *meso*-erythritol, (E) xylitol, and (F) sorbitol. Symbols represent experimental melting temperatures (squares), eutectic temperatures (circles) and other transitions (triangles), measured using the visual or oil bath method (open symbols) or DSC (black symbols), and data Abranches *et al.* (red square),[19] Silva *et al.* (green diamond),[28] and Abbott *et al.* (green cross).[61] The *x*-axis is the mole fraction of betaine or choline chloride. Lines represent the ideal model of betaine (black dashed line), the polyol and choline chloride (green dashed line), and the polyol normal boiling temperature (dotted line). The melting properties of choline chloride were T_m = 597 K, ΔH_m = 4.3 kJ mol^{-1}.[15] Coloured regions represent the concentration range of a stable monophasic liquid phase at room temperature of the betaine (gray) and choline chloride (green) mixtures.

deviations observed in betaine mixtures can be attributed to carboxylate cross-interactions with hydroxyl groups, which are not possible in pure betaine. An exception to the trend for ChCl is seen in the glycerol mixture, where slight negative deviations from ideality are observed for ChCl.

COSMO-RS also markedly captures the difference between the interactions ChCl – polyols and betaine – polyols, predicting negative deviations for betaine and near-ideal behaviour (or even positive deviations) for ChCl. That difference can also be seen in Fig. S2, which shows the isothermal activity coefficients for both sets of systems at 300 K and 400 K.

Among the polyols, glycerol, *meso*-erythritol, xylitol, and sorbitol exhibit negative deviations from ideality in ChCl mixtures, while ethylene glycol and 1,3-propanediol display near-

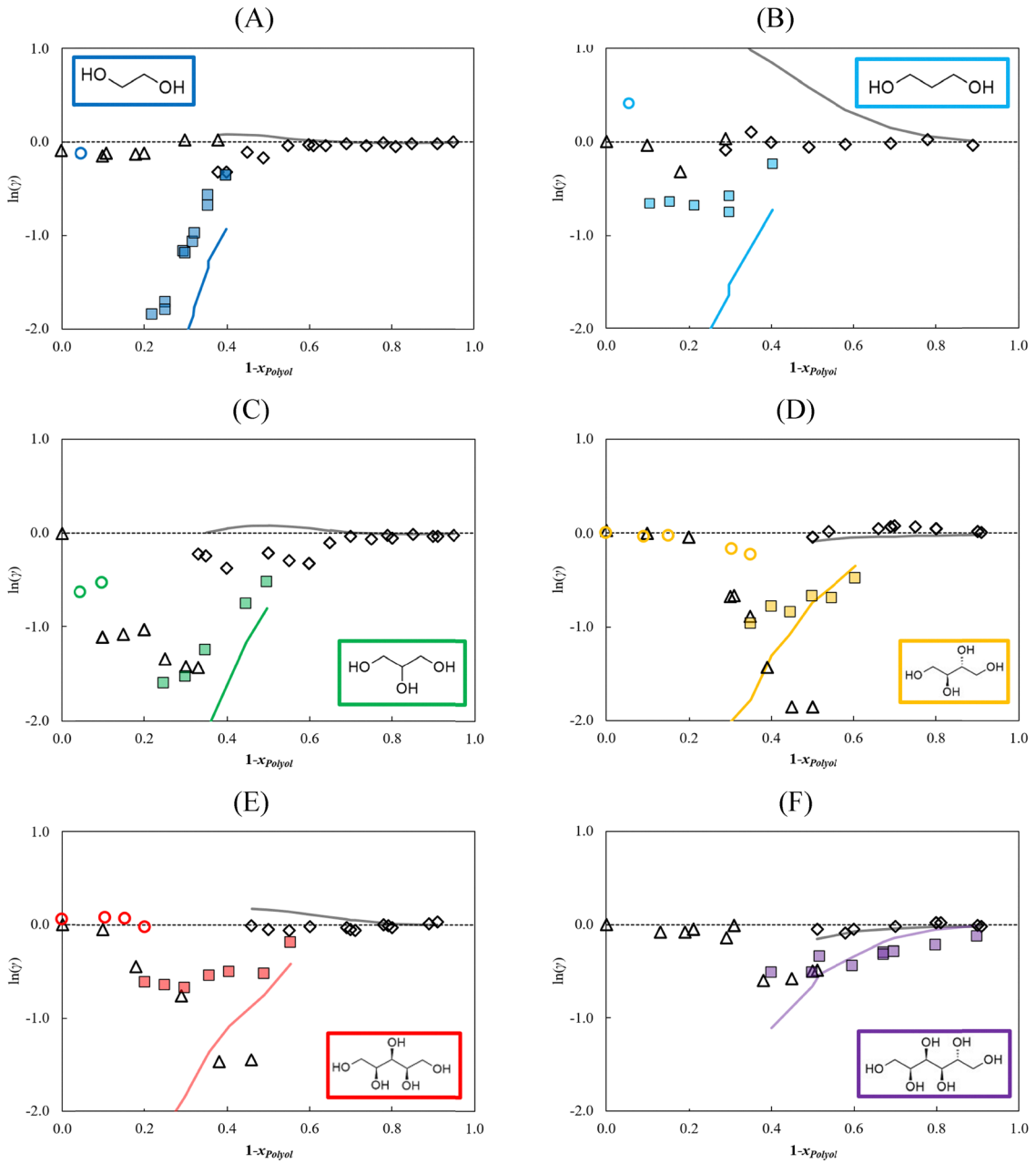

Fig. 5 Non-isothermal activity coefficients of betaine and choline chloride and (A) ethylene glycol, (B) 1,3-propanediol, (C) glycerol, (D) *meso*-erythritol, (E) xylitol, and (F) sorbitol. Symbols represent the activity coefficients of betaine (colored squares) with polyol (colored circle), and choline chloride (black diamond) with polyol (black triangle). Data on betaine/sorbitol and choline chloride mixture are adapted from literature.[19,28] Dotted lines represent the ideal behaviour, $\ln(\gamma_i) = 0$. Solid lines represent COSMO-RS (TZVPD-FINE parametrization): ChCl (black lines) and betaine (other colored lines).

ideal behaviour. As discussed,[28] these deviations can be attributed to the cross-interaction mentioned earlier (polyol hydroxyl group with the chloride anion). Since the former four polyols have more hydroxyl groups than the latter two, there are more instances in which these interactions form, leading to more negative deviations.[28] Moreover, there is a limit for these interactions, as *meso*-erythritol presents lower activity coefficients than xylitol and sorbitol, as the latter polyols present more hydroxyl groups than the former.[28] Meanwhile, the same four polyols presented near-ideal behaviour in betaine mixtures. The systems with ethylene glycol and 1,3-propanediol showed a narrow concentration range over which their solid phases form; however, because of cocrystal formation with betaine, ethylene glycol is expected to exhibit significant negative deviations.

Based on the results above, there is no indication that the behaviour of polyols in the presence of ChCl differs significantly from that observed with betaine. Rather, the lower melting enthalpy of ChCl leads to eutectic points at higher HBA compositions. This, in turn, broadens the liquidus curves

of polyols, extending them into intermediate composition ranges where deviations from ideal behaviour become more pronounced. Accordingly, polyols are also expected to exhibit similar negative deviations when mixed with betaine.

4. Conclusion

This study examined mixtures of natural compounds (polyols and betaine) to characterize their phase behaviour and assess their potential as deep eutectic solvents. The SLE phase diagrams were measured across most of the composition range using three different experimental techniques. However, the complete composition range could not be determined due to the boiling points of the polyols and/or the thermal degradation of betaine. Additionally, the high viscosity of some polyols prevented the recrystallization of the mixtures. In general, betaine showed negative deviations from ideality, while most polyols exhibited near-ideal behaviour.

Using both experimental results and COSMO-RS predictions, betaine was found to exhibit substantial negative deviations from ideality, associated with stronger cross-interactions between polyols and betaine than betaine–betaine interactions. Importantly, this conclusion was found to be robust with respect to the numerical value of the enthalpy of fusion of betaine, which is not available from direct experimental measurements due to the decomposition of betaine upon melting.

The SLE behaviour of betaine–polyol systems was further studied by replacing betaine with ChCl, a popular HBA choice in the literature. Rather interestingly, in contrast to betaine, a much lower level of non-ideality was observed for ChCl. Nevertheless, the liquidus line of ChCl was consistently lower (*i.e.*, at lower temperatures) than the liquidus line of betaine. The fact that (i) betaine displays negative deviations from ideality, while ChCl does not, and (ii) the liquidus temperatures of ChCl are consistently lower than the liquidus temperatures of betaine implies that the melting enthalpy of ChCl must be lower than that of betaine. In fact, taking this argument further, it implies that the melting enthalpy of ChCl cannot exceed the lower bound melting enthalpy of betaine, estimated in this work to be 12 kJ mol^{-1}.

The COSMO-RS predictions for the systems studied in this work are very satisfactory considering the uncertainty associated with the melting enthalpy of betaine. Further insights into molecular interactions and conformers could be gained through density functional theory (DFT) calculations and Fourier-transform Raman spectroscopy. This work also highlights the critical role of water in betaine mixtures, as even small amounts can significantly influence their phase behaviour.

Conflicts of interest

There are no conflicts of interest to declare.

Data availability

The data supporting this article including the experimental solid–liquid equilibrium data have been included as part of the supplementary information (SI). Supplementary information: Fig. S1–S4 and Tables S1–S6. See DOI: https://doi.org/10.1039/d6cp00104a.

Acknowledgements

This work was developed within the scope of the projects CICECO - Aveiro Institute of Materials, UID/50011/2025 (https://doi.org/10.54499/UID/50011/2025) & LA/P/0006/2020 (https://doi.org/10.54499/LA/P/0006/2020); CIMO UID/00690/2025 (https://doi.org/10.54499/UID/00690/2025) e UID/PRR/00690/2025 (https://doi.org/10.54499/UID/PRR/00690/2025); SusTEC, LA/P/0007/2020 (https://doi.org/10.54499/LA/P/0007/2020); CIQUP, Faculty of Science, University of Porto (Project UIDB/00081/2025), and IMS – Institute of Molecular Sciences (https://doi.org/10.54499/LA/P/0056/2020) financed by national funds through the Portuguese Foundation for Science and Technology FCT/MCTES (PIDDAC). G.T. thanks FCT for his PhD grant (UI/BD/151114/2021).

References

1 M. A. R. Martins, S. P. Pinho and J. A. P. Coutinho, Insights into the Nature of Eutectic and Deep Eutectic Mixtures, *J. Solution Chem.*, 2019, **48**, 962–982.
2 D. O. Abranches and J. A. P. Coutinho, Everything You Wanted to Know about Deep Eutectic Solvents but Were Afraid to Be Told, *Annu. Rev. Chem. Biomol. Eng.*, 2023, **14**, 141–163.
3 E. L. Smith, A. P. Abbott and K. S. Ryder, Deep Eutectic Solvents (DESs) and Their Applications, *Chem. Rev.*, 2014, **114**, 11060–11082.
4 F. Oyoun, A. Toncheva, L. C. Henríquez, R. Grougnet, F. Laoutid, N. Mignet, K. Alhareth and Y. Corvis, Deep Eutectic Solvents: An Eco-friendly Design for Drug Engineering, *ChemSusChem*, 2023, **16**, e202300669.
5 D. Rente, M. Cvjetko Bubalo, M. Panić, A. Paiva, B. Caprin, I. Radojčić Redovniković and A. R. C. Duarte, Review of deep eutectic systems from laboratory to industry, taking the application in the cosmetics industry as an example, *J. Cleaner Prod.*, 2022, **380**, 135147.
6 A. T. H. Yeow, A. Hayyan, M. Hayyan, M. Usman Mohd Junaidi, J. Saleh, W. Jefrey Basirun, M. Roslan Mohd Nor, W. Al Abdulmonem, M. Zulhaziman, M. Salleh, F. Mohamed Zuki and M. Diana Hamid, A comprehensive review on the physicochemical properties of deep eutectic solvents, *Results Chem.*, 2024, **7**, 101378.
7 P. A. Shah, V. Chavda, D. Hirpara, V. S. Sharma, P. S. Shrivastav and S. Kumar, Exploring the potential of deep eutectic solvents in pharmaceuticals: Challenges and opportunities, *J. Mol. Liq.*, 2023, **390**, 123171.
8 M. S. Rahman, R. Roy, B. Jadhav, M. N. Hossain, M. A. Halim and D. E. Raynie, Formulation, structure, and

applications of therapeutic and amino acid-based deep eutectic solvents: An overview, *J. Mol. Liq.*, 2021, **321**, 114745.
9 M. Liu, D. Cao, W. Bi and D. D. Y. Chen, Extraction of Natural Products by Direct Formation of Eutectic Systems, *ACS Sustainable Chem. Eng.*, 2021, **9**, 12049–12057.
10 D. Cao, Q. Liu, W. Jing, H. Tian, H. Yan, W. Bi, Y. Jiang and D. D. Y. Chen, Insight into the Deep Eutectic Solvent Extraction Mechanism of Flavonoids from Natural Plant, *ACS Sustainable Chem. Eng.*, 2020, **8**, 19169–19177.
11 B. Tang, H. Zhang and K. H. Row, Application of deep eutectic solvents in the extraction and separation of target compounds from various samples, *J. Sep. Sci.*, 2015, **38**, 1053–1064.
12 I. F. Mena, E. Diaz, J. Palomar, J. J. Rodriguez and A. F. Mohedano, Cation and anion effect on the biodegradability and toxicity of imidazolium– and choline–based ionic liquids, *Chemosphere*, 2020, **240**, 124947.
13 M. Marchel, H. Cieśliński and G. Boczkaj, Thermal Instability of Choline Chloride-Based Deep Eutectic Solvents and Its Influence on Their Toxicity—Important Limitations of DESs as Sustainable Materials, *Ind. Eng. Chem. Res.*, 2022, **61**, 11288–11300.
14 K. Radošević, M. Cvjetko Bubalo, V. Gaurina Srček, D. Grgas, T. Landeka Dragičević and I. Radojčić Redovniković, Evaluation of toxicity and biodegradability of choline chloride based deep eutectic solvents, *Ecotoxicol. Environ. Saf.*, 2015, **112**, 46–53.
15 L. Fernandez, L. P. Silva, M. A. R. Martins, O. Ferreira, J. Ortega, S. P. Pinho and J. A. P. Coutinho, Indirect assessment of the fusion properties of choline chloride from solid-liquid equilibria data, *Fluid Phase Equilib.*, 2017, **448**, 9–14.
16 S. M. Vilas-Boas, D. O. Abranches, E. A. Crespo, O. Ferreira, J. A. P. Coutinho and S. P. Pinho, Experimental solubility and density studies on aqueous solutions of quaternary ammonium halides, and thermodynamic modelling for melting enthalpy estimations, *J. Mol. Liq.*, 2020, **300**, 112281.
17 G. B. Correa, D. O. Abranches, E. Marin-Rimoldi, Y. Zhang, E. J. Maginn and F. W. Tavares, Assessing Melting and Solid-Solid Transition Properties of Choline Chloride via Molecular Dynamics Simulations, *J. Phys. Chem. Lett.*, 2024, 11801–11805.
18 A. van den Bruinhorst, J. Avila, M. Rosenthal, A. Pellegrino, M. Burghammer and M. Costa Gomes, Defying decomposition: the curious case of choline chloride, *Nat. Commun.*, 2023, **14**, 6684.
19 D. O. Abranches, L. P. Silva, M. A. R. Martins, S. P. Pinho and J. A. P. Coutinho, Understanding the Formation of Deep Eutectic Solvents: Betaine as a Universal Hydrogen Bond Acceptor, *ChemSusChem*, 2020, **13**, 4916–4921.
20 R. A. Kozlovsky, V. F. Shvets and M. G. Makarov, A Kinetic Model of the Choline Chloride Synthesis, *Org. Process Res. Dev.*, 1999, **3**, 357–362.
21 S. Wang, Y. Zhang and J. Wang, Solubility Measurement and Modeling for Betaine in Different Pure Solvents, *J. Chem. Eng. Data*, 2014, **59**, 2511–2516.
22 B. B. Hansen, S. Spittle, B. Chen, D. Poe, Y. Zhang, J. M. Klein, A. Horton, L. Adhikari, T. Zelovich, B. W. Doherty, B. Gurkan, E. J. Maginn, A. Ragauskas, M. Dadmun, T. A. Zawodzinski, G. A. Baker, M. E. Tuckerman, R. F. Savinell and J. R. Sangoro, Deep Eutectic Solvents: A Review of Fundamentals and Applications, *Chem. Rev.*, 2021, **121**, 1232–1285.
23 R. Wahlström, J. Hiltunen, M. Pitaluga de Souza Nascente Sirkka, S. Vuoti and K. Kruus, Comparison of three deep eutectic solvents and 1-ethyl-3-methylimidazolium acetate in the pretreatment of lignocellulose: effect on enzyme stability, lignocellulose digestibility and one-pot hydrolysis, *RSC Adv.*, 2016, **6**, 68100–68110.
24 M. Panić, V. Gunjević, G. Cravotto and I. Radojčić Redovniković, Enabling technologies for the extraction of grape-pomace anthocyanins using natural deep eutectic solvents in up-to-half-litre batches extraction of grape-pomace anthocyanins using NADES, *Food Chem.*, 2019, **300**, 125185.
25 P. Zhou, X. Wang, P. Liu, J. Huang, C. Wang, M. Pan and Z. Kuang, Enhanced phenolic compounds extraction from Morus alba L. leaves by deep eutectic solvents combined with ultrasonic-assisted extraction, *Ind. Crops Prod.*, 2018, **120**, 147–154.
26 S. Khodaverdian, B. Dabirmanesh, A. Heydari, E. Dashtbanmoghadam, K. Khajeh and F. Ghazi, Activity, stability and structure of laccase in betaine based natural deep eutectic solvents, *Int. J. Biol. Macromol.*, 2018, **107**, 2574–2579.
27 H. Wang, S. Liu, Y. Zhao, J. Wang and Z. Yu, Insights into the Hydrogen Bond Interactions in Deep Eutectic Solvents Composed of Choline Chloride and Polyols, *ACS Sustainable Chem. Eng.*, 2019, **7**, 7760–7767.
28 L. P. Silva, M. A. R. Martins, J. H. F. Conceição, S. P. Pinho and J. A. P. Coutinho, Eutectic Mixtures Based on Polyalcohols as Sustainable Solvents: Screening and Characterization, *ACS Sustainable Chem. Eng.*, 2020, **8**, 15317–15326.
29 F. Eckert and A. Klamt, Fast Solvent Screening via Quantum Chemistry: COSMO-RS Approach, *AIChE J.*, 2002, **48**, 369–385.
30 A. Kovács, E. C. Neyts, I. Cornet, M. Wijnants and P. Billen, Modeling the Physicochemical Properties of Natural Deep Eutectic Solvents, *ChemSusChem*, 2020, **13**, 3789–3804.
31 D. O. Abranches, M. Larriba, L. P. Silva, M. Melle-Franco, J. F. Palomar, S. P. Pinho and J. A. P. Coutinho, Using COSMO-RS to design choline chloride pharmaceutical eutectic solvents, *Fluid Phase Equilib.*, 2019, **497**, 71–78.
32 D. S. Raut, V. A. Joshi, S. Khan and D. Kundu, A-Priori screening of deep eutectic solvent for enhanced oil recovery application using COSMO-RS framework, *J. Mol. Liq.*, 2023, **377**, 121482.
33 G. S. Parks and K. K. Kelley, Thermal data on organic compounds. ii. the heat capacities of five organic compounds. the entropies and free energies of some homologous series of aliphatic compounds, *J. Am. Chem. Soc.*, 1925, **47**, 2089–2097.
34 K. Takeda, O. Yamamuro, I. Tsukushi, T. Matsuo and H. Suga, Calorimetric study of ethylene glycol and 1,3-propanediol:

configurational entropy in supercooled polyalcohols, *J. Mol. Struct.*, 1999, **479**, 227–235.
35 S. Jabrane, J. M. Létoffé and P. Claudy, Study of the thermal behaviour of 1,3-propanediol and its aqueous solutions, *Thermochim. Acta*, 1998, **311**, 121–127.
36 W. E. Acree, Thermodynamic properties of organic compounds: enthalpy of fusion and melting point temperature compilation, *Thermochim. Acta*, 1991, **189**, 37–56.
37 M. Volmer and M. Marder, Zur Theorie der linearen Kristallisationsgeschwindigkeit unterkühlter Schmelzen und unterkühlter fester Modifikationen, *Z. Phys. Chem.*, 1931, **154A**, 97–112.
38 M. C. Righetti, G. Salvetti and E. Tombari, Heat capacity of glycerol from 298 to 383K, *Thermochim. Acta*, 1998, **316**, 193–195.
39 A. J. Lopes Jesus, L. I. N. Tomé, M. E. Eusébio and J. S. Redinha, Enthalpy of Sublimation in the Study of the Solid State of Organic Compounds. Application to Erythritol and Threitol, *J. Phys. Chem. B*, 2005, **109**, 18055–18060.
40 M. E. Spaght, S. B. Thomas and G. S. Parks, Some Heat-Capacity Data on Organic Compounds obtained with a Radiation Calorimeter, *J. Phys. Chem.*, 1932, **36**, 882–888.
41 E. S. Domalski and E. D. Hearing, Heat Capacities and Entropies of Organic Compounds in the Condensed Phase. Volume III, *J. Phys. Chem. Ref. Data*, 1996, (25), 1–525.
42 B. Tong, Z.-C. Tan, Q. Shi, Y.-S. Li, D.-T. Yue and S.-X. Wang, Thermodynamic investigation of several natural polyols (I): Heat capacities and thermodynamic properties of xylitol, *Thermochim. Acta*, 2007, **457**, 20–26.
43 B. Tong, Z. C. Tan, Q. Shi, Y. S. Li and S. X. Wang, Thermodynamic investigation of several natural polyols (II), *J. Therm. Anal. Calorim.*, 2008, **91**, 463–469.
44 J. A. P. Coutinho, S. I. Andersen and E. H. Stenby, Evaluation of activity coefficient models in prediction of alkane solid-liquid equilibria, *Fluid Phase Equilib.*, 1995, **103**, 23–39.
45 A. Klamt, Conductor-like Screening Model for Real Solvents: A New Approach to the Quantitative Calculation of Solvation Phenomena, *J. Phys. Chem.*, 1995, **99**, 2224–2235.
46 A. Klamt, V. Jonas, T. Bürger and J. C. W. Lohrenz, Refinement and parametrization of COSMO-RS, *J. Phys. Chem. A*, 1998, **102**, 5074–5085.
47 D. O. Abranches and J. A. P. Coutinho, Type V Deep Eutectic Solvents: Design and Applications, *Curr. Opin. Green Sustainable Chem.*, 2022, 100612.
48 M. Diedenhofen and A. Klamt, COSMOconf. COSMOlogic, Leverkusen, Germany, 2008, preprint.
49 TURBOMOLE V7.4 2019, a development of University of Karlsruhe and Forschungszentrum Karlsruhe GmbH, 1989-2007, TURBOMOLE GmbH, since 2007; available from https://www.turbomole.com.
50 S. G. Balasubramani, G. P. Chen, S. Coriani, M. Diedenhofen, M. S. Frank, Y. J. Franzke, F. Furche, R. Grotjahn, M. E. Harding, C. Hättig, A. Hellweg, B. Helmich-Paris, C. Holzer, U. Huniar, M. Kaupp, A. Marefat Khah, S. Karbalaei Khani, T. Müller, F. Mack, B. D. Nguyen, S. M. Parker, E. Perlt, D. Rappoport, K. Reiter, S. Roy, M. Rückert, G. Schmitz, M. Sierka, E. Tapavicza, D. P. Tew, C. van Wüllen, V. K. Voora, F. Weigend, A. Wodyński and J. M. Yu, TURBOMOLE: Modular program suite for *ab initio* quantum-chemical and condensed-matter simulations, *J. Chem. Phys.*, 2020, **152**, 184107.
51 BIOVIA COSMOtherm, Release 2021, Dassault Systèmes.
52 A. Mero, S. Koutsoumpos, P. Giannios, I. Stavrakas, K. Moutzouris, A. Mezzetta and L. Guazzelli, Comparison of physicochemical and thermal properties of choline chloride and betaine-based deep eutectic solvents: The influence of hydrogen bond acceptor and hydrogen bond donor nature and their molar ratios, *J. Mol. Liq.*, 2023, **377**, 121563.
53 H. Palmelund, B. J. Boyd, J. Rantanen and K. Löbmann, Influence of water of crystallization on the ternary phase behavior of a drug and deep eutectic solvent, *J. Mol. Liq.*, 2020, **315**, 113727.
54 A. Alhadid, C. Jandl, S. Nasrallah, S. M. Kronawitter, L. Mokrushina, G. Kieslich and M. Minceva, Estimating the nonideality of eutectic systems containing thermally unstable substances, *J. Chem. Phys.*, 2023, **159**, 094503.
55 P. Kavuru, D. Aboarayes, K. K. Arora, H. D. Clarke, A. Kennedy, L. Marshall, T. T. Ong, J. Perman, T. Pujari, Ł. Wojtas and M. J. Zaworotko, Hierarchy of Supramolecular Synthons: Persistent Hydrogen Bonds Between Carboxylates and Weakly Acidic Hydroxyl Moieties in Cocrystals of Zwitterions, *Cryst. Growth Des.*, 2010, **10**, 3568–3584.
56 J. F. Carson, S. W. Waisbrot and F. T. Jones, A New Form of Crystalline Xylitol, *J. Am. Chem. Soc.*, 1943, **65**, 1777–1778.
57 I. Zahrina, K. Mulia, A. Yanuar and M. Nasikin, Molecular interactions in the betaine monohydrate-polyol deep eutectic solvents: Experimental and computational studies, *J. Mol. Struct.*, 2018, **1158**, 133–138.
58 R. Politi, L. Sapir and D. Harries, The Impact of Polyols on Water Structure in Solution: A Computational Study, *J. Phys. Chem. A*, 2009, **113**, 7548–7555.
59 I. Zahrina, M. Nasikin, K. Mulia, M. Prajanto and A. Yanuar, Molecular interactions between betaine monohydrate-glycerol deep eutectic solvents and palmitic acid: Computational and experimental studies, *J. Mol. Liq.*, 2018, **251**, 28–34.
60 D. O. Abranches, L. P. Silva, M. A. R. Martins and J. A. P. Coutinho, Differences on the impact of water on the deep eutectic solvents betaine/urea and choline/urea, *J. Chem. Phys.*, 2021, **155**(3), 034501.
61 A. P. Abbott, P. M. Cullis, M. J. Gibson, R. C. Harris and E. Raven, Extraction of glycerol from biodiesel into a eutectic based ionic liquid, *Green Chem.*, 2007, **9**, 868.